Coupling Mechanisms of Sustainable Daily Vitality and Resilient Disaster Recovery in Flood-Prone High-Density Urban Areas

Zhihao Shen[1], Yu Yan[1], Shilin Wei[1], Yating Fan[1,2*]

[1]School of Architecture and Urban Planning, Shenzhen University, Shenzhen, 518060, Guangdong, China
[2]State Key Laboratory of Subtropic Building and Urban Science (Shenzhen University), Shenzhen, 518060, Guangdong, China

Abstract: With the intensification of global climate change, frequent extreme weather events have exerted significant impacts on urban built environments and residents' lives. Strengthening urban resilience is therefore essential for disaster prevention and mitigation. Existing research has primarily focused on either vitality or recovery, which limits systematic understanding of disaster evolution. Investigating the coupling and coordination between daily vitality and Disaster Recovery is crucial for integrated urban disaster assessment and optimization. This study takes the 2023 extreme rainfall event in South China as the case and the Guanlan River Basin in Shenzhen as the study area. Based on mobile signaling data, an evaluation framework was constructed across three dimensions—urban recovery, vitality, and disaster–peace coupling coordination—to measure and assess the compound urban resilience of land parcels. Building on this framework, K-means clustering was employed to identify typical land parcel types, and spatial autocorrelation was applied to reveal the degree of spatial clustering of the indicators. Finally, regression models were used to investigate the underlying mechanisms of built environment factors influencing these indicators. The results indicate that Sustainable Daily Vitality and Resilient Disaster Recovery exhibit strong spatial correlation, with substantial variations in indicator values among land parcels according to their functional characteristics. These indicators are also largely influenced by built environment factors, including road configuration, building density, and service facilities. This study contributes to clarifying the development of resilience mechanisms in high-density cities and provides a reference for exploring the mechanisms of integrated urban disaster–resilience development.

1. Introduction

Flooding is one of the most devastating natural hazards worldwide, often causing significant economic losses and human casualties[1]. With the intensification of global climate change and the continuous expansion of urban built-up areas, meteorological disasters—particularly extreme events such as heavy rainfall and urban waterlogging—pose serious threats to the safety of urban areas[2,3]. Data from 2023 indicate that China experienced extreme and abnormal climatic events, with multiple river basins suffering severe floods. The total direct economic losses nationwide reached 62 billion RMB, representing an increase of approximately 29.4% compared with the average of the previous three years[4]. Traditional urban infrastructure and construction models are increasingly inadequate for coping with current flood challenges[5], highlighting the need for resilient city planning and integrated disaster–resilience development as new approaches for urban flood prevention and mitigation.

Urban resilience is widely regarded as the capacity of a system to respond to disasters, recover from them, absorb their impacts, and adapt to a new normal[6]. To assess the extent of flood damage in urban built-up areas and to investigate the disaster-related mechanisms of the built environment, the evaluation of urban flood resilience has become a major research focus. Resilience curves drawn according to the disaster process are generally divided into four stages: early warning, resistance, recovery, and adaptation, which together describe the overall impact of disruptive events on the system[7]. Among them, the recovery and adaptation stages correspond to the Resilient Disaster Recovery and Sustainable Daily Vitality of land parcels, respectively. If an urban built-up area can rapidly recover from disruptive events and shift from a disaster state to a normal state[8], while maintaining strong and active internal system connections, the land parcels within it are considered to possess high Resilient Disaster Recovery and Sustainable Daily Vitality.

Numerous studies have explored methods for evaluating Sustainable Daily Vitality and Resilient Disaster Recovery, yet most have examined them separately. In terms of assessing urban daily vitality, traditional approaches have primarily relied on field surveys, face-to-face interviews, and questionnaires[9]. With the rapid development of information and communication technologies, multi-source big data have increasingly replaced traditional data collection methods

* Corresponding author: fyt_fighting@szu.ed.cn

as research data sources. For example, heat map data[10,11], social media check-in records[12,13], location-based review data[14], and mobile signaling data [9,15] enable the measurement of urban spatial vitality at finer scales and with unprecedented volumes of information. For the evaluation of Resilient Disaster Recovery, disaster loss data are typically collected through field surveys, satellite imagery, unmanned aerial vehicles (UAVs)[16,17], or social media data[18]. However, these approaches face limitations in accurately capturing the extent to which human activities are affected by disasters. The evaluation of Resilient Disaster Recovery based on mobile signaling data[19] offers high accuracy, broad coverage, and rapid processing, and has therefore been widely adopted in research. However, existing studies have paid limited attention to assessing the Vitality–Recovery Coupling Coordination Degree or to evaluating corresponding integrated disaster reduction strategies.

In this study, mobile signaling data were used to calculate the Sustainable Daily Vitality–Resilient Disaster Recovery indices for the Guanlan River Basin in Shenzhen. By integrating multiple existing methods for assessing recovery and vitality, this approach can accurately estimate, based on changes in population density captured by mobile signaling data, the recovery efficiency, daily vitality level, and their Vitality–Recovery Coupling Coordination Degree of different urban land parcels following extreme rainfall and flood events. Building on this framework, K-means clustering and spatial autocorrelation models were applied to investigate the distribution patterns and spatial clustering of the Sustainable Daily Vitality–Resilient Disaster Recovery indices across urban land parcels. These results provide a clearer understanding and assessment of the Vitality–Recovery Coupling Coordination Degree of different parcels. In addition, regression models were employed to analyze the relationships between built environment factors and the Sustainable Daily Vitality–Resilient Disaster Recovery indices. This approach enables the identification of weak links and areas in integrated urban disaster–resilience development, providing methods and recommendations for enhancing urban flood resilience.

2. Materials and Methods

2.1. Overview of Study Area

Shenzhen is located in South China, on the eastern shore of the Guangdong–Hong Kong–Macao Greater Bay Area. The city has a subtropical monsoon climate, with an average annual precipitation of 1,935.8 mm, of which 86% occurs during the flood season (April–September). The period from July to September is the peak typhoon season, with the city typically struck by 4–5 typhoons annually, making it highly prone to extreme weather events. Shenzhen has 310 rivers, among which the five largest are the Shenzhen River, Maozhou River, Guanlan River, Longgang River, and Pingshan River. Owing to its unique geographical location and rapid urbanization, the city's hydrological conditions have undergone significant changes over the past decades. As a result, extreme rainfall has frequently triggered urban flooding[20], causing considerable economic losses and social challenges. As show in figures 1 and 2.

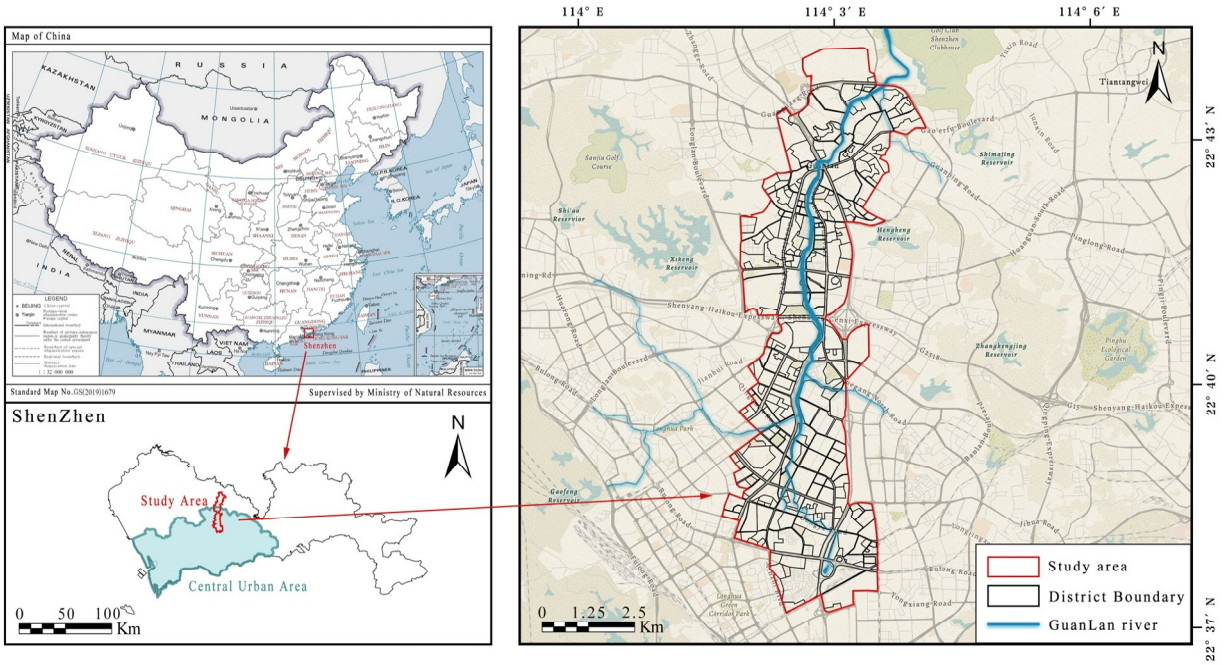

Fig. 1. Location of the study area.

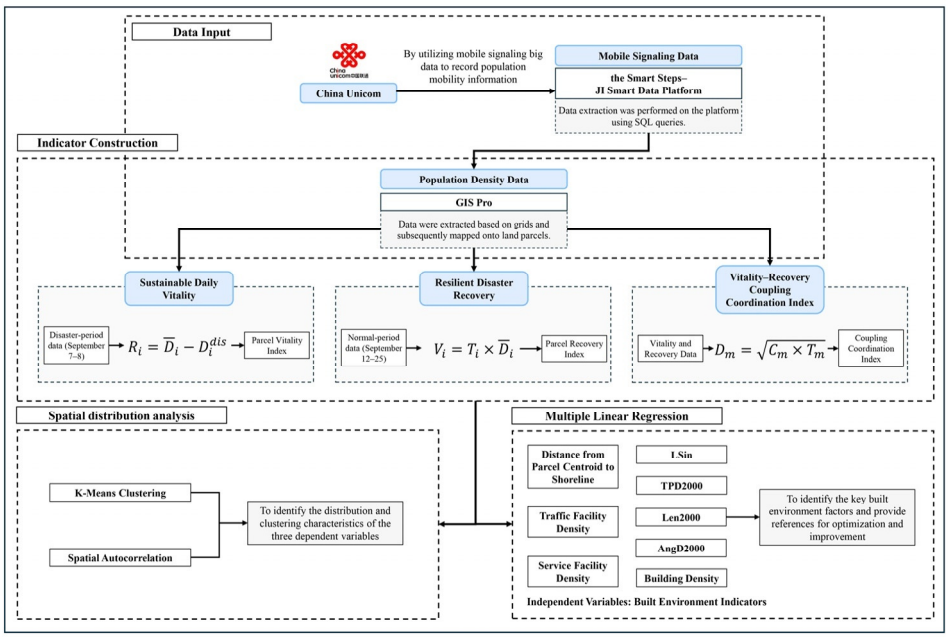

Fig. 2. Framework of the Study.

Influenced by the residual circulation of Typhoon Haikui (No. 2311), together with monsoon activity and cold air, Shenzhen experienced record-breaking extreme rainfall from 17:00 on September 7 to 15:30 on September 8, 2023[21]. This event resulted in severe flooding in several river basins, including the Longgang River, Shenzhen River, and Guanlan River. Based on this, the section of the Guanlan River in Shenzhen between Guangguang Road and Bulong Road, which was severely affected by the typhoon, was selected as the study area. The study area covers a river section of approximately 13.67 km in length, with a 1,000 m buffer zone extending into the hinterland on both sides of the riverbank. Based on the functional attributes contained in the POI data of land parcels, the study divides the research area into 328 independent "functional parcels." Furthermore, the functional types are categorized into six groups: public service land, public space land, commercial and office land, residential land, industrial land, and other land. Within the study area, the functional distribution of land parcels exhibits a clear north–south differentiation. The northern parcels retain the original road network, where residential and industrial areas are intermingled, and include traditional settlements such as the Guanlan Old Market, reflecting a rich historical legacy. In contrast, the southern parcels have been shaped by urban planning, featuring a more regular road network with concentrations of industrial zones and high-end residential communities, as well as facilities such as the Foxconn campus and a water purification plant. Consequently, the land parcels within the selected area display heterogeneous built environment characteristics and face diverse challenges in relation to flooding.

2.2. Data Sources and Preprocessing

This study utilizes signaling data from the Unicom's Smart Footprint big data Platform (JI Smart) to comprehensively evaluate Sustainable Daily Vitality and post-disaster resilience within the study area. Owing to its high accuracy and density, the dataset effectively captures population activity patterns during disaster events[22], particularly reflecting dynamic behaviors in high-density urban centers.

Based on publicly available news reports and hourly precipitation data, this study reconstructed the event timeline of the study area. A continuous 19-day period was selected as the observation window for data analysis and subsequently divided into two stages. As the heaviest rainfall occurred on September 7 and 8, gradually decreasing in intensity, this study defines these two days (September 7–8) as the disaster period, reflecting the system's transition from resistance to recovery. From the fourth day after the event, September 12, the system began to stabilize. The following 14 days (September 12–25) are defined as the stable period, representing the system's internal stability and daily activity under normal conditions.

By spatially overlaying the study area with the platform's 150 × 150 m grids, data within each grid were extracted on an hourly basis. Using an area-weighted aggregation method based on the relationship between the research land parcels and the grids, this study constructed a parcel-level network system capturing the spatiotemporal dynamics of the urban population. Missing values or unreasonable extreme values resulting from calculations were screened and replaced with more plausible data to ensure continuity. Since the processed mobile signaling data represent the number of people per hour within each land parcel, magnitude differences exist between parcels. To eliminate these differences, the data were normalized by dividing the population by the parcel area. The calculation formula is as follows:

$$D_i = \frac{P_i}{A_i} \quad (1)$$

This formula calculates the population density of each land parcel, where D_i represents the population density of parcel i, P_i denotes the number of people, and A_i is the area of the parcel.

2.3. Indicator System Construction

The process by which urban built-up areas withstand floods is complex and diverse, and numerous indicators have been proposed by scholars for measurement[23,24]. Based on the stages of disaster occurrence, this study categorizes the evaluation indicators into three dimensions: Resilient Disaster Recovery, Sustainable Daily Vitality, and the Vitality–Recovery Coupling Coordination Degree. These factors are essential for assessing the disaster–peace integration of urban built environments and provide guidance for post-disaster improvement and optimization.

2.3.1 Sustainable Daily Vitality Evaluation Indicators

For the measurement of urban vitality indicators, numerous studies have constructed indicators from different perspectives and approaches. For example, street vitality has been evaluated through street-view image recognition[25]; population density within street areas derived from mobile signaling data has been used to represent vitality[26,27]; and urban street vitality has been assessed using built environment and POI data[28]. These approaches have been widely validated by researchers as feasible and effective methods of measurement.

Mobile signaling data were extracted to measure parcel vitality. Specifically, the average daily population density of each parcel from the 5th day after the disaster (12th) to the 25th day was compared with the 14-day mean value for the same period. The number of days exceeding the 14-day mean was recorded and multiplied by the 14-day mean to serve as the vitality indicator of each parcel. Counting the days above the 14-day mean allows a better assessment of the magnitude and trend of population density variation: a larger number of days indicates more stable post-disaster population density changes within the parcel, whereas fewer days suggest that parcel vitality is mainly influenced by outliers on a limited number of days. The calculation formula for the vitality evaluation indicator of each parcel is expressed as follows:

$$V_i = T_i \times \overline{D}_i \tag{2}$$

This formula measures the parcel vitality indicator, where V_i denotes the vitality value, T_i represents the number of days on which the average daily population density of parcel i exceeds its 14-day mean, and $\overline{D}_i$ denotes the 14-day average population density of parcel i.

2.3.2 Resilient Disaster Recovery Evaluation Indicators

For the calculation of urban recovery capacity indicators, researchers have adopted various perspectives and approaches. For instance, urban resilience has been measured using the integral equation of resilience curves[19,29,30]; resilience assessment has been conducted by analyzing disaster-related information collected from social media data[18,31]; and recovery has been evaluated through the variation time and rate of resilience curves[29].

Population density information derived from mobile signaling data was used to calculate recovery. The disaster event was defined as occurring on September 7 and 8, and the average population density of each parcel on these two days was computed as the disaster-period data. The difference between the disaster-period data and the previously calculated 14-day mean was then calculated, and the resulting value was used as the parcel recovery indicator. The calculation formula for the recovery evaluation indicator of each parcel is presented as follows:

$$R_i = \overline{D}_i - D_i^{dis} \tag{3}$$

This formula measures the parcel recovery indicator, where R_i denotes the recovery capacity, $\overline{D}_i$ represents the 14-day average population density of the parcel, and D_i^{dis} denotes the average population density of the parcel during the two disaster days.

2.3.3 Vitality–Recovery Coupling Evaluation Indicators

Parcel Sustainable Daily Vitality reflects the level of population aggregation under normal conditions, whereas Resilient Disaster Recovery represents the ability to recover after disaster impacts. Together, these two dimensions characterize the state of urban spaces during the disaster–peace transition, which is critical for assessing the "disaster–peace integration" of parcels. Therefore, in this study, the Vitality–Recovery Coupling Coordination Degree [32] was calculated to evaluate the conflict and synergy between vitality and recovery, providing a comprehensive assessment of parcel performance within urban resilience.

The coupling degree (C) is calculated using the following formula:

$$C = 2 \times \left[\frac{V \times R}{(V+R)^2}\right]^{\frac{1}{2}} \tag{4}$$

Where C represents the coupling degree between vitality and recovery, with $C \in [0,1]$. A higher C value indicates a stronger interaction between the two indicators. V and R denote vitality and recovery, respectively. The coordination index (T) is calculated as follows:

$$T = \beta_1 V + \beta_2 R \tag{5}$$

Where T denotes the coordination index between vitality and recovery, calculated as the sum of the weighted indices of the two indicators. In this study, vitality and recovery are considered equally important, thus $\beta_1 = \beta_2 = \frac{1}{2}$. The coupling coordination degree combines the coupling degree and the coordination index

to assess the level of coordinated development, and is calculated using the following formula:

$$D_m = \sqrt{C_m \times T_m} \quad (6)$$

Where D_m represents the Vitality–Recovery Coupling Coordination Degree, C_m denotes the coupling degree between vitality and recovery,and T_m represents the coordination index of vitality and recovery.

2.4. Spatial Autocorrelation and K-means Clustering Analysis

Spatial autocorrelation evaluates the differences or similarities between neighboring spatial values through statistical methods, thereby revealing the spatial clustering or dispersion of disaster–peace integration in urban blocks[33]. Local spatial autocorrelation (LISA model) further refines this analytical process by identifying differences in disaster–peace integration from a local perspective. K-means clustering is a classical local distance-based unsupervised algorithm that partitions data automatically by minimizing the squared error between each sample point and its assigned cluster center[34]. In this study, the K-means algorithm was applied to cluster Sustainable Daily Vitality, Resilient Disaster Recovery, and the Vitality–Recovery Coupling Coordination Degree in order to identify areas with similar characteristics.

2.5. OLS Model for Identifying Built Environment Factors

This study constructed a multiple linear regression model using the stepwise method. Independent variables were sequentially introduced into the model according to their relative influence on the dependent variable, thereby identifying the impact coefficients of each factor. The regression equation was estimated using the ordinary least squares (OLS) method.

Urban Resilient Disaster Recovery and Sustainable Daily Vitality are significantly associated with the built environment. For example, the expansion of impervious surfaces during urban growth prolongs the infiltration time of surface runoff, thereby increasing the frequency of flooding events[35,36]. In addition, higher building density and reduced green space can affect both the extent of disaster impact on urban parcels and their recovery efficiency. This study focuses on the Guanlan River area in Shenzhen and selects built environment variables that are closely related to stormwater and population dynamics[37]. To reduce the impact of multicollinearity on the model, the variables were selected based on a VIF test and include: building density, distance from the parcel centroid to the shoreline, transportation facilities density, service facilities density, LSin (road curvature), TPD2000 (weighted road accessibility within 2,000 meters), Len2000 (total road length within 2,000 meters), and AngD2000 (path tortuosity within 2,000 meters). By constructing linear regression models between eight categories of built environment indicators and parcel Resilient Disaster Recovery and Sustainable Daily Vitality, this study reveals the influencing mechanisms of different types of built environment factors and provides guidance for targeted optimization and improvement of the urban built environment.

3. Results

In order to examine the vitality and resilience levels of urban parcels, the calculated indicator values were normalized.

To clearly present and interpret the normalized results, the data for Sustainable Daily Vitality, Resilient Disaster Recovery, and the Vitality–Recovery Coupling Coordination Degree were divided into five categories: high, slightly high, medium, slightly low, and low. Among various classification methods available in GIS Pro, the natural breaks (Jenks) method was selected. This method, commonly used in cartography and spatial statistical analysis, classifies data based on natural clustering patterns, maximizing similarity within groups while enhancing differences between groups. This approach ensures scientific grouping and provides an accurate and effective strategy for classification. Therefore, the natural breaks method was adopted for data categorization in this study.

3.1. Distribution of Sustainable Daily Vitality, Resilient Disaster Recovery, and Coupling Coordination Degree

3.1.1 Distribution of Urban Parcel Sustainable Daily Vitality

The urban vitality index, which measures the stability of daily urban activity, was classified into five categories in this study using the natural breaks method.

As shown in Figure 3a, the parcel Sustainable Daily Vitality in the study area is predominantly medium and low, with a clear north–south differentiation. High-value areas are relatively concentrated, particularly in the southern part of the region. Hotspot analysis further reveals that this area contains significant vitality hotspots, where parcel functions are mainly factories and high-end residential zones. Overall, the northern parcels exhibit noticeably lower vitality values and are primarily distributed along the river in a scattered pattern. The formation of low-value areas along the river indicates that, under the traditional village layout, roads are largely aligned along the river and closely interact with it, while inter-regional traffic connectivity remains limited. Comparative analysis shows that the Sustainable Daily Vitality index of river-adjacent parcels in the northern region is only about 1/5 to 1/10 of that in the southern region, representing a 5- to 10-fold difference. In the central area, large-scale transportation facilities hinder connectivity between parcels, resulting in generally low vitality levels and the formation of regional cold spots. In contrast, the southern region, influenced by parcel functions, features well-organized urban roads and convenient transportation, supporting strong population mobility and adequate infrastructure, leading to extensive

areas with high vitality values. Based on spatial form and functional attributes, the spatial differentiation of the parcel Sustainable Daily Vitality index is likely influenced by a combination of factors, including land-use type, building density, and road accessibility. Among these, road accessibility and the functional diversity of parcels may be key drivers for the formation of high-value areas in the southern region.

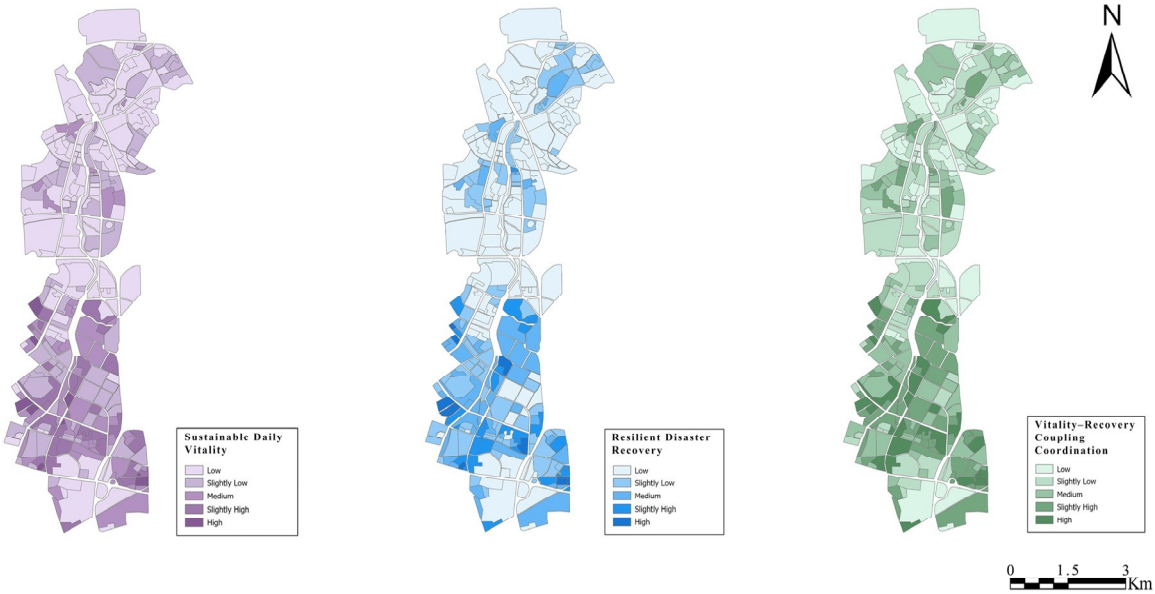

Fig. 3. Spatial Distribution and Characteristics of the Indicators.

3.1.2 Distribution of Urban Parcel Resilient Disaster Recovery

The parcel Resilient Disaster Recovery index, which measures the ability of a parcel to transition from disaster conditions to normal conditions, is typically associated with factors such as infrastructure and road accessibility. In this study, the data were classified into five categories using the natural breaks method.

As shown in Figure 3b, the distribution of the parcel Resilient Disaster Recovery index is generally similar to that of the vitality index. High-value areas are concentrated in the southern region, while the northern region exhibits scattered slightly higher values, and the central region is predominantly low-value. Hotspot analysis reveals that the southern region forms significant recovery hotspots, though their distribution is relatively dispersed, exhibiting a multi-centered clustering pattern. In contrast, the extensive low-value areas in the central region represent recovery cold spots, primarily influenced by impediments from transportation facilities and homogeneous land-use functions.

Overall, the spatial clustering of the slightly higher-value areas in the northern region is more pronounced than that of the vitality distribution, showing a radial diffusion pattern along the river. However, compared with the high-value areas in the southern region, the recovery index of northern parcels remains relatively low, approximately 1/2 to 1/3 of the southern values, indicating a significant north–south disparity. Further comparison reveals that the north–south difference in the vitality index reaches 5–10 times, far exceeding that of the recovery index. This discrepancy may reflect differences in their spatial formation mechanisms: vitality levels are more directly influenced by population mobility, industry types, and the aggregation effects of parcel functions, resulting in a clear "amplification effect" of market and social activities in the southern core area; in contrast, recovery relies more heavily on the road network, infrastructure, and the level of public services. Based on parcel functions and morphological characteristics, the spatial differentiation of the Resilient Disaster Recovery index is likely influenced by multiple factors, including land-use type, infrastructure level, road accessibility, and the density of socio-economic activities. Among these, the integrity of the transportation network and the functional diversity of parcels may be key drivers for the formation of high-value areas in the southern region.

3.1.3 Distribution of Urban Parcel Vitality–Recovery Coupling Coordination Degree

The Vitality–Recovery Coupling Coordination Degree index, which measures the synergy between vitality and recovery, is crucial for evaluating the disaster–peace integration of parcels. In this study, the data were classified into five categories using the natural breaks method.

As shown in Figure 3c, compared with the individual indicators of vitality and recovery, the Vitality–Recovery Coupling Coordination Degree exhibits a more balanced north–south distribution, with a dominant trend in the southern region. The proportion of low-value areas is greatly reduced, indicating that vitality and recovery are relatively well-coordinated across most parcels, with both systems not only performing well individually but also developing synchronously. High-value areas are more extensively distributed in the southern region, suggesting that this area has a certain degree of functional diversity,

well-developed infrastructure, and high road accessibility, thus possessing comprehensive capabilities for both daily vitality and emergency recovery. Medium and slightly low-value areas are widely distributed in the central region, indicating that the ecosystem is gradually integrating into the urban resilience framework. In the northern region, high-value areas are scattered, highlighting the need for improvement and restoration of traditional road networks and construction patterns within the context of resilient urban development.

3.2. Cluster Intensity and Pattern Characteristics Analysis

3.2.1 K-means Clustering Analysis

Using parcel-level indicators of Daily Sustainable Vitality and Resilient Disaster Recovery as clustering variables, the K-means algorithm was applied to classify the study area. The analysis divided the samples into four distinct categories, characterized by high intra-group cohesion and significant inter-group differences.

As shown in Figure 4, the clustering patterns are primarily characterized by H–H and L–L types, while H–L and L–H combinations are relatively rare. This distribution may be attributed to the fact that parcels with high daily vitality tend to exhibit strong clustering effects, which in turn enhance their emergency response capacity during disasters and support more robust recovery performance. Overall, the VH–VH pattern indicates parcels with exceptionally high values for both indicators, but accounts for only about 2% of the sample. The H–H pattern represents approximately 11% of the parcels, primarily located in the southern high-end electronics industrial parks and upscale residential areas. The M–M pattern makes up about 26%, with scattered distributions in both the southern and northern parts of the study area. The L–L pattern constitutes the largest share at roughly 62%, predominantly distributed across northern urban villages and traditional industrial parks.

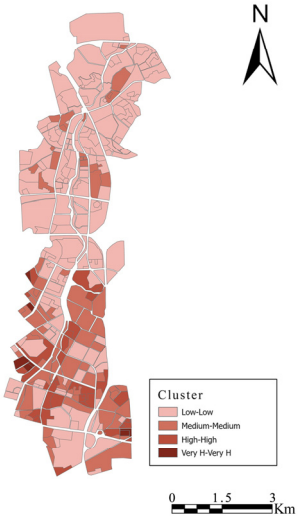

Fig. 4. K-means Clustering Distribution.

This north–south spatial differentiation is likely closely related to industrial and residential functions. In the south, electronics industrial parks benefit from industrial agglomeration that fosters strong innovation and capital orientation. Combined with well-developed infrastructure and higher levels of public resource allocation, these areas can mobilize and recover quickly during disasters, thus exhibiting the H–H clustering pattern. By contrast, northern traditional industrial parks are constrained by a monocultural industrial structure, lagging spatial renewal, and insufficient public service facilities, which result in the prevalence of the L–L pattern under disaster impacts.

3.2.2 Spatial Autocorrelation Analysis

Global and local spatial autocorrelation analyses were conducted on the indicators of Sustainable Daily Vitality, Resilient Disaster Recovery, and their coupling coordination, effectively detecting the spatial clustering patterns of each indicator. The results of the local spatial autocorrelation analysis are presented in Figure 5.

The analysis results indicate that the Moran's I values for all indicators are greater than 0, indicating a moderately strong positive spatial autocorrelation and suggesting that the indicators exhibit spatial clustering. The significance level ($p < 0.01$) further confirms the robustness of the results. This implies that the levels of Sustainable Daily Vitality, Resilient Disaster Recovery, and the Vitality–Recovery Coupling Coordination Degree tend to be similar among neighboring parcels, reflecting a clear spatial clustering effect.

As shown in the LISA cluster map (Figure 5), a clear north–south differentiation in clustering patterns is observed. The northern part is dominated by L–L clusters, with scattered H–L outlier parcels, indicating that both vitality and recovery remain at low levels, forming a large-scale low-value agglomeration zone. In contrast, the southern part is characterized primarily by H–H clusters, suggesting a significant advantage in both Resilient Disaster Recovery and Sustainable Daily Vitality. Scattered L–H outlier parcels also appear, reflecting localized deficiencies in composite resilience despite being embedded in high-level surrounding contexts.

In the H–H clustering zones of Resilient Disaster Recovery, the Guanlan River demonstrates a pronounced agglomeration effect, highlighting the close association between urban recovery and waterfront spaces. As an ecological and open-space carrier, the river enhances the recovery potential of parcels and strengthens the self-organizing capacity of the urban system. In the L–L clustering zones of Sustainable Daily Vitality, the northern part of the study area forms a low-vitality "depression," suggesting that limited road accessibility, functional composition, and development intensity jointly constrain urban vitality. The clustering patterns of the coupling coordination degree largely align with the distributions of vitality and recovery. Accordingly, future urban renewal and refined governance should prioritize improving infrastructure, promoting functional integration, and advancing resilience-oriented urban

construction in the northern areas. The presence of scattered L–H outlier parcels in the southern region further indicates deficiencies in composite resilience, underscoring the need to strengthen integrated resilience planning to ensure rapid response and system stability under sudden disturbances.

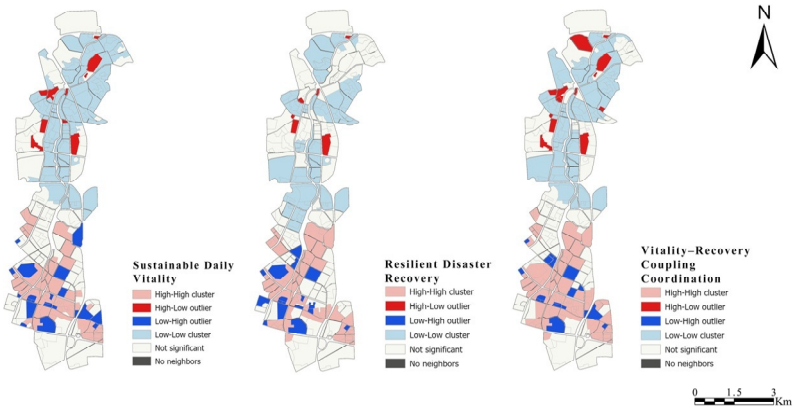

Fig. 5. Spatial Clustering Analysis of the Study Area.

Table 1. Statistical Result of Linear Regression Independent Variable Coefficients

Dependent variable	Resilient Disaster Recovery		Sustainable Daily Vitality		Coupling Coordination Degree	
Independent Variable	**Beta**	**P**	**Beta**	**P**	**Beta**	**P**
Len2000	0.608	<0.001	0.584	<0.001	0.697	<0.001
Service Facility Density	0.374	<0.001	0.285	<0.001	0.337	<0.001
Building Density	–	–	0.137	0.006	0.156	0.001
Lsin	–	–	0.144	0.005	0.140	0.004
Transportation Facility Density	-0.190	<0.001	–	–	-0.131	0.007
TPD2000	-0.201	0.003	-0.273	<0.001	-0.316	<0.001
AngD2000	-0.255	<0.001	-0.289	<0.001	-0.354	<0.001

3.3. Attribution Analysis of Differences in Vitality–Recovery Coupling

In this study, Sustainable Daily Vitality, Resilient Disaster Recovery, and the Vitality–Recovery Coupling Coordination Degree were treated as dependent variables, while parcel-level built environment indicators served as independent variables. The data were applied to linear regression models to quantify and interpret the effects of the independent indicators. The results are presented in Table 1, where Beta represents the standardized coefficient in the regression equation, with its magnitude reflecting the relative influence on the dependent variable. The sign indicates the direction of the effect, while the significance test (p) ensures the statistical reliability of the results.

In the regression model for Resilient Disaster Recovery, five indicators were found to have significant effects, with an adjusted R^2 of 0.345, indicating a reasonably good fit. Among these, service facility density ($B = 0.297$, $p < 0.001$), transportation facility density ($B = –0.210$, $p < 0.001$), and Len2000 ($B = 0.392$, $p < 0.001$) exhibited the strongest explanatory power, highlighting their critical roles in Resilient Disaster Recovery ; For Sustainable Daily Vitality, six independent variables were included in the regression model, with an adjusted R^2 of 0.356, slightly higher than that of the recovery model. Service facility density ($B = 0.288$, $p < 0.001$), Len2000 ($B = 0.48$, $p < 0.001$), and TPD2000 ($B = –0.235$, $p < 0.001$) exerted the strongest influences on vitality. Additionally, building density ($B = 0.122$, $p = 0.006$) was incorporated into the model, indicating that the morphological characteristics of the built environment play an important role in shaping urban vitality ; For the Vitality–Recovery Coupling Coordination Degree, seven independent variables were included in the regression model, with an adjusted R^2 of 0.444. Service facility density ($B = 0.302$, $p < 0.001$), Len2000 ($B = 0.506$, $p < 0.001$), and TPD2000 ($B = –0.239$, $p < 0.001$) remained the primary influencing factors, indicating their central role in the coupling coordination model. The higher goodness-of-fit compared with the previous two models suggests that the coupling coordination degree, as an indicator simultaneously measuring vitality and recovery, can better explain the disaster–peace integration level of urban parcels. The study also notes that in the regression model, the independent variables Transportation Facility Density and TPD2000 show negative correlations with all dependent variables, whereas Len2000 and Lsin exhibit positive correlations. This suggests that excessive traffic facility density and road accessibility may lead to block fragmentation and redundant road networks, thereby weakening vitality, resilience, and coupling coordination. In contrast, greater road length and curvature may correspond to a more organic street network structure, which is more conducive to post-disaster recovery and the enhancement of daily vitality.

Overall, the comparison of the three models highlights the superiority of the coupling coordination degree indicator: it not only integrates the dual characteristics of vitality and recovery but also demonstrates a higher

goodness-of-fit compared with single-variable models. By emphasizing the importance of incorporating composite indicators in disaster resilience research, this study provides a more reliable quantitative basis for urban disaster prevention and planning.

4. Discussion

This study established a comprehensive evaluation framework from three perspectives: Resilient Disaster Recovery [38,39], Sustainable Daily Vitality [40,41], and the Vitality–Recovery Coupling Coordination Degree[42,43], aiming to characterize urban resilience under natural disasters such as flooding. Using the natural breaks method in GIS, the development patterns of disaster–peace integration in the parcels of the Guanlan River basin in Shenzhen were assessed. Furthermore, spatial statistical analyses were conducted on the urban parcel evaluation system. The Local Indicators of Spatial Association (LISA) model [33] and K-means clustering [34] were applied to reveal spatial clustering patterns of Resilient Disaster Recovery, Sustainable Daily Vitality, and their coupling coordination. In addition, to identify the key factors influencing disaster impacts, linear regression models were employed, integrating hydrological environment and built environment variables to analyze the main determinants of urban flood resistance and recovery. Through these approaches, the study not only uncovers the spatial heterogeneity of multidimensional characteristics within the study area but also provides empirical support for understanding the mechanisms affecting high-density urban floodplains under disaster conditions.

Previous studies on urban Resilient Disaster Recovery [44] and Sustainable Daily Vitality [45] have mostly treated these two indicators separately, with limited systematic analysis of their interrelationships. In addition, most research on urban recovery and vitality tends to focus on ecological [33,46] or social media perspectives[47], which cannot accurately capture population mobility under disaster conditions, thereby constraining dynamic analyses of urban responses, resilience, and recovery in high-density cities. To address this limitation, this study utilizes mobile signaling data to construct novel indicators from a big-data perspective, enabling real-time and rapid reflection of spatial patterns of population movement. This study further examines their relationships with built environment factors, such as building density, public facility distribution, and road accessibility. In this way, this study more accurately captures the resilience characteristics of urban systems under disaster impacts, providing a scientific basis for urban planning and disaster prevention strategies, and promoting coordinated optimization in disaster–peace integration and urban development.

Regarding strategies for enhancing urban resilience, numerous studies and city planners have proposed effective improvement measures and recommendations. At the community scale, replacing impervious pavements with permeable surfaces and improving urban drainage through engineering interventions can mitigate urban flooding. For example, the recently discussed green infrastructure disaster–peace integration design [48] can act as flood retention during disasters, thereby enhancing urban recovery, while simultaneously serving as public activity space under normal conditions to promote urban vitality. This approach is considered one of the effective ways to improve the urban ecological environment[49–51]. At the planning level, establishing robust early warning systems and leveraging big data to build grid-based statistical monitoring systems can realize “smart water management” [33]. Overall, improvements in urban disaster–peace integration should be comprehensive and coordinated from multiple perspectives, aiming to create ecologically friendly and resilient urban districts.

In summary, this study constructed an urban disaster–peace integration measurement system for city districts using mobile signaling data. However, several limitations remain. The processing of mobile signaling data did not account for differences in population attributes, such as residents, workers, or visitors within each parcel. In addition, the identification of disaster-affected parcels was not explicitly addressed, and for some parcels, weekend population fluctuations exceeded those caused by the disaster. Future research will consider refining population categories and identifying significantly affected parcels to better assess trends in disaster impacts on both land and population. Moreover, by selecting different types of indicators for different study areas, the research can achieve broader applicability.

5. Conclusion

This study assessed the disaster–peace integration development level of selected parcels within the Guanlan River basin in Shenzhen, using a system of indicators based on Resilient Disaster Recovery, Sustainable Daily Vitality, and the Vitality–Recovery Coupling Coordination Degree to evaluate the comprehensive performance of urban districts under heavy rainfall and flooding. This assessment provides an intuitive and effective quantitative method for evaluating overall urban development. The main findings are summarized as follows:

(1) High values of urban vitality and recovery are predominantly observed in the southern part of the study area, where parcel functions are diverse and transportation is convenient, whereas the northern area, consisting of traditional historical districts, exhibits lower levels of both vitality and recovery.

(2) Indicators such as road morphology, building density, and service facility density have significant positive effects on urban district vitality and recovery. The coupling coordination degree, which has been less discussed in previous research, provides a more comprehensive model with higher explanatory power.

(3) The spatial clustering pattern of disaster–peace integration in the districts is mainly characterized by H-H and L-L clusters, with few parcels exhibiting low vitality–high recovery or high vitality–low recovery.

Future research on urban flood disaster prevention, early warning, and recovery should integrate multi-source

data and adopt a multi-dimensional approach to accurately and comprehensively assess urban resilience under heavy rainfall and inland flooding.

Acknowledgement

This research was supported by the National Natural Science Foundation of China (52308026), the Guangdong Province Natural Science Foundation (2023A1515011274), and the Shenzhen Municipal Stable Support Plan for Higher Education Institutions (20231122150425001).

References

1. Agrawal N, Elliott M and Simonovic S 2020 Risk and Resilience: A Case of Perception versus Reality in Flood Management *Water* **12** 1254
2. Leichenko R 2011 Climate change and urban resilience *Current Opinion in Environmental Sustainability* **3** 164–8
3. Adediran I A, Isah K O, Ogbonna A E and Badmus S K 2023 A Global Analysis of the Macroeconomic Effects of Climate Change *Asian Economics Letters* **4**
4. HUO C, WANG K, and GAO L 2023 National flood and drought disaster prevention in China in 2023 *China Flood & Drought Management* **33** 1–4
5. Xia J, Zhang Y, Xiong L, He S, Wang L and Yu Z 2017 Opportunities and challenges of the Sponge City construction related to urban water issues in China *Sci. China Earth Sci.* **60** 652–8
6. Saravi S, Kalawsky R, Joannou D, Rivas Casado M, Fu G and Meng F 2019 Use of Artificial Intelligence to Improve Resilience and Preparedness Against Adverse Flood Events *Water* **11** 973
7. Tang J, Zhao P, Gong Z, Zhao H, Huang F, Li J, Chen Z, Yu L and Chen J 2023 Resilience patterns of human mobility in response to extreme urban floods *National Science Review* **10** nwad097
8. Zhong M, Lin K, Tang G, Zhang Q, Hong Y and Chen X 2020 A Framework to Evaluate Community Resilience to Urban Floods: A Case Study in Three Communities *Sustainability* **12** 1521
9. Chen Y, Yu B, Shu B, Yang L and Wang R 2023 Exploring the spatiotemporal patterns and correlates of urban vitality: Temporal and spatial heterogeneity *Sustainable Cities and Society* **91** 104440
10. Zhou C, Fu L, Xue Y, Wang Z and Zhang Y 2022 Using multi-source data to understand the factors affecting mini-park visitation in Yancheng *Environment and Planning B: Urban Analytics and City Science* **49** 754–70
11. Yang J 2021 Elaborating non-linear associations and synergies of subway access and land uses with urban vitality in Shenzhen
12. Ouyang J, Fan H, Wang L, Zhu D and Yang M 2022 Revealing urban vibrancy stability based on human activity time-series *Sustainable Cities and Society* **85** 104053
13. Qin S, Yang J, Feng Y and Yan S 2021 Spatiotemporal vitality and influencing factors of urban parks based on multi-source data: A case study of Nanjing *Chin. Landsc. Archit* **37** 68–73
14. Meng Y and Xing H 2019 Exploring the relationship between landscape characteristics and urban vibrancy: A case study using morphology and review data *Cities* **95** 102389
15. [15] LUO S, ZHANG Z, YANG Z, and LUO X 2024 Study on the Spatial and Temporal Characteristics and Influencing Factors of Vitality of Urban Waterfront Parks: A Case Study Based on Kunming City *South Architecture/Nanfang Jianzhu* 69–77
16. Rahman Md M, Siddique S, Kamal M, Rifat R H and Gupta K D 2024 UAV (Unmanned Aerial Vehicle): Diverse Applications of UAV Datasets in Segmentation, Classification, Detection, and Tracking *Algorithms* **17** 594
17. Ullah F, Khan S I, Munawar H S, Qadir Z and Qayyum S 2021 UAV Based Spatiotemporal Analysis of the 2019–2020 New South Wales Bushfires *Sustainability* **13** 10207
18. Hao H and Wang Y 2020 Leveraging multimodal social media data for rapid disaster damage assessment *International Journal of Disaster Risk Reduction* **51** 101760
19. Anon Resilience patterns of human mobility in response to extreme urban floods
20. Han J-C, Zheng W, Liu Z, Zhou Y, Huang Y and Li B 2022 Downscaling of Precipitation for Climate Change Projections Using Multiple Machine Learning Techniques: Case Study of Shenzhen City, China *J. Water Resour. Plann. Manage.* **148**
21. SONG L, CHEN J and LIU Z 2024 Retrospective simulation and analysis on "9· 7" extraordinary rainstorm and flood in the Shenzhen City: taking the Guanlan watershed of the Longhua District as an example *China Flood & Drought Management* **34** 19–23
22. Yang L, Liang Y, He B, Yang H and Lin D 2023 COVID-19 moderates the association between to-metro and by-metro accessibility and house prices *Transportation Research Part D: Transport and Environment* **114** 103571
23. Keating A, Campbell K, Szoenyi M, McQuistan C, Nash D and Burer M 2016 Development and testing of a community flood resilience measurement tool
24. Liang Y, Wang C, Chen G and Xie Z 2024 Evaluation framework ACR-UFDR for urban form disaster resilience under rainstorm and flood scenarios: A case study in Nanjing, China *Sustainable Cities and Society* **107** 105424
25. Bai Z, Huang S, Wang L and Qi J 2025 Refined understanding of street vitality: comparing the spatial effects of pedestrian vitality and cycling vitality and

the spatial heterogeneity of factors *International Journal of Digital Earth* **18** 2501769

26. Guo X, Chen H and Yang X 2021 An Evaluation of Street Dynamic Vitality and Its Influential Factors Based on Multi-Source Big Data *IJGI* **10** 143
27. Yue Y, Zhuang Y, Yeh A G O, Xie J-Y, Ma C-L and Li Q-Q 2017 Measurements of POI-based mixed use and their relationships with neighbourhood vibrancy *International Journal of Geographical Information Science* **31** 658–75
28. Li M, Liu J, Lin Y, Xiao L and Zhou J 2021 Revitalizing historic districts: Identifying built environment predictors for street vibrancy based on urban sensor data *Cities* **117** 103305
29. Yan X, Pei T, Gong X, Fu Z and Liu Y 2025 Assessing differences in work intensity resilience to pandemic outbreaks using large-scale mobile phone data *International Journal of Applied Earth Observation and Geoinformation* **136** 104343
30. [30] Hong B, Bonczak B J, Gupta A and Kontokosta C E 2021 Measuring inequality in community resilience to natural disasters using large-scale mobility data *Nat Commun* **12** 1870
31. Huang X, Li Z, Wang C and Ning H 2020 Identifying disaster related social media for rapid response: a visual-textual fused CNN architecture *International Journal of Digital Earth* **13** 1017–39
32. Lin Y, Peng C, Chen P and Zhang M 2022 Conflict or synergy? Analysis of economic-social-infrastructure-ecological resilience and their coupling coordination in the Yangtze River economic Belt, China *Ecological Indicators* **142** 109194
33. Zhou M, He Q, Gu Y, Wang K and Shen Z 2025 Urban Flood Resilience Assessment of Prefecture-Level Cities in Yangtze River Delta *IJGI* **14** 108
34. MacQueen J 1967 Multivariate observations *Proceedings ofthe 5th Berkeley Symposium on Mathematical Statisticsand Probability* vol 1 pp 281–97
35. Chen A S, Hammond M J, Djordjević S, Butler D, Khan D M and Veerbeek W 2016 From hazard to impact: flood damage assessment tools for mega cities *Nat Hazards* **82** 857–90
36. Miller J D, Kim H, Kjeldsen T R, Packman J, Grebby S and Dearden R 2014 Assessing the impact of urbanization on storm runoff in a peri-urban catchment using historical change in impervious cover *Journal of Hydrology* **515** 59–70
37. Lee Y and Brody S D 2018 Examining the impact of land use on flood losses in Seoul, Korea *Land Use Policy* **70** 500–9
38. Li H, Han Y, Wang X and Li Z 2024 Risk perception and resilience assessment of flood disasters based on social media big data *International Journal of Disaster Risk Reduction* **101** 104249
39. Zhang X, Mao F, Gong Z, Hannah D M, Cai Y and Wu J 2023 A disaster-damage-based framework for assessing urban resilience to intense rainfall-induced flooding *Urban Climate* **48** 101402
40. Zhang R, Jiang A and Jiang L 2025 Exposure-Sensitivity-Adaptability (ESA) framework based evaluation and characteristics analysis of urban disasters vulnerability in China *Ecological Indicators* **176** 113662
41. Chen Z, Dong B, Pei Q and Zhang Z 2022 The impacts of urban vitality and urban density on innovation: Evidence from China's Greater Bay Area *Habitat International* **119** 102490
42. Ji J, Chen J F, Ding T H, and Li Y H 2024 Coupling coordination between urban flood resilience and ecosystem services in the Yangtze River Delta urban agglomerations *Acta Ecologica Sinica* **44** 2772–85
43. Ji J, Chen J, Ding T and Gu Y 2025 How to achieve coordinated and sustainable development between urban flood resilience and ecosystem services at the urban agglomeration scale *Journal of Environmental Management* **388** 126010
44. Li H, Han Y, Wang X and Li Z 2024 Risk perception and resilience assessment of flood disasters based on social media big data *International Journal of Disaster Risk Reduction* **101** 104249
45. Bai Z, Huang S, Wang L and Qi J 2025 Refined understanding of street vitality: comparing the spatial effects of pedestrian vitality and cycling vitality and the spatial heterogeneity of factors *International Journal of Digital Earth* **18** 2501769
46. LI Y, WANG M, and WANG Y 2025 The Concept, Quantitative Measurement, and Spatial Differentiation of Urban Spatial Vulnerability: A Case Study of Prefecture-level Cities in the ChengduChongqing Economic Circle *Urban Planning Forum* 43–50
47. Tang J, Yang S and Wang W 2021 Social media-based disaster research: Development, trends, and obstacles *International Journal of Disaster Risk Reduction* **55** 102095
48. FAN Y and ZHANG M 2024 Research Prospects on Urban Water-sensitive Open Space and its Infrastructure for Dual-use of Disaster and Routine: Using Emerging Urban Ergonomics Data *World Architecture Review* **39** 52–7
49. Lee H, Song K, Kim G and Chon J 2021 Flood-adaptive green infrastructure planning for urban resilience *Landscape Ecol Eng* **17** 427–37
50. Chen W, Wang W, Huang G, Wang Z, Lai C and Yang Z 2021 The capacity of grey infrastructure in urban flood management: A comprehensive analysis of grey infrastructure and the green-grey approach *International Journal of Disaster Risk Reduction* **54** 102045
51. Li L, Uyttenhove P and Van Eetvelde V 2020 Planning green infrastructure to mitigate urban surface water flooding risk – A methodology to identify priority areas applied in the city of Ghent *Landscape and Urban Planning* **194** 103703